JOURNAL OF THERMOPHYSICS AND HEAT TRANSFER
Vol. 11, No. 2, April–June 1997

Influence of Buoyancy on Convective Heat Transfer in Helicoidal Pipes

R. C. Xin* and M. A. Ebadian†
Florida International University, Miami, Florida 33199

The combined effects of curvature and buoyancy forces on convective heat transfer in axially vertical and horizontal helicoidal pipes have been explored in this investigation. Distilled water and ethylene glycol were used as working fluids. It has been observed that natural convection causes the peripheral maximum Nusselt number location to shift from the outer coil wall to the bottom of the tube cross section in the vertical coil. In the horizontal coil, the axial temperature distribution becomes periodically wavy with the presence of natural convection. The three following heat transfer regimes have been observed from the local temperature and Nusselt number distributions in the experiment of vertical helicoidal pipes: 1) a regime in which centrifugal force is dominant, 2) a regime in which both the centrifugal and buoyancy forces are effective (mixed regime), and 3) a regime in which the buoyancy force is dominant. Furthermore, it has been found that natural convection enhances heat transfer significantly for high Prandtl number fluids (e.g., ethylene glycol), but its effect is minor on the average Nusselt number for low Prandtl number fluids (e.g., water).

Nomenclature

A = correlation constant
b = coil pitch, m
D_c = diameter of the coil centerline, m
De = Dean number, $Re(d/D_c)^{1/2}$
d = pipe diameter, m
g = gravitational acceleration, m/s^2
k = thermal conductivity, W/(m °C)
L = length of one turn in the helicoidal pipe, m
Nu = Nusselt number, Eq. (7)
$\overline{Nu}$ = peripheral average Nusselt number
q'' = input heat flux, W/m^2
Ra = Rayleigh number, $g\beta q'' d^4/(k\nu^2) \times Pr$
Re = Reynolds number, $\rho U_m d/\mu$
T = temperature, °C
U = axial velocity, m/s
Z = dimensionless axial distance
z = axial distance, m
β = coefficient of thermal expansion, 1/°C
ΔT_m = mean temperature difference, °C
δ = deviation
θ = dimensionless axial wall temperature distribution, Eq. (4)
μ = fluid dynamic viscosity, kg/(s m)
ρ = fluid density, kg/m^3
ν = fluid kinematic viscosity, m^2/s
ψ = peripheral angle
ψ_0 = correlation constant

Subscripts
b = bulk
c = coil
i = inner wall
in = inlet
m = mean value
o = outer wall
out = outlet
w = wall
z = value at z location
ψ = peripheral local value

Received July 10, 1996; revision received Dec. 6, 1996; accepted for publication Dec. 10, 1996.

*Research Associate, Hemispheric Center for Environmental Technology. Member AIAA.
†Professor and Director, Hemispheric Center for Environmental Technology. Member AIAA.

Introduction

HEAT exchangers constructed of curved tubes and coils are of interest in many industrial applications, including compact heat exchangers and chemical processes. In addition to their wide use in industry, curved and helicoidal pipes have also been applied to the field of biomedical instruments and diagnostics. It is well known that centrifugal and buoyancy forces produce secondary flow, which causes a higher streamwise pressure gradient, a higher critical Reynolds number for transition to turbulent flow, and higher average heat and mass transfer coefficients compared to those for flow in straight pipes without secondary flow.

A review of the literature indicates that many experimental, theoretical, and numerical investigations on both fluid flow and heat transfer inside curved and helicoidal pipes have been conducted. The research on fluid flow inside curved pipes has been summarized by Berger and Talbot.[1] Many experimental and theoretical studies on convective heat transfer in circular curved and helicoidal pipes have also been reported.[2–6] Manlapaz and Churchill[7] derived the following equation by performing a regression analysis on the available Nusselt number results for laminar flow in helicoidal pipes with constant heat flux boundary conditions:

$$Nu = \left\{ \left[4.364 + \frac{4.636}{1 + 1342/(De^2 Pr)^2} \right]^3 + 1.816 \left(\frac{De}{1 + 1.15/Pr} \right)^{3/2} \right\}^{1/3} \tag{1}$$

For turbulent flow with the same boundary condition, Gnielinski's correlation[8] is widely used for its generality:

$$Nu = \frac{(f/8)RePr}{1 + 12.7\sqrt{f/8}(Pr^{2/3} - 1)} \left(\frac{Pr}{Pr_w} \right)^{0.14} \tag{2}$$

where the friction factor f is calculated by the equation:

$$f = \left[\frac{0.3164}{Re^{0.25}} + 0.03\left(\frac{d}{De}\right)^{0.5}\right]\left(\frac{\mu_w}{\mu}\right)^{0.27} \quad (3)$$

The previous correlations have been used as the bases for an analysis of the effect of the buoyancy force on heat transfer. For helicoidal pipes, coil pitch introduces another parameter in addition to the coil-to-tube diameter ratio D_c/d. A systematic experimental investigation of the effect of coil pitch on forced convection was reported by Austen and Soliman.[9] Some deviations of heat transfer with different coil pitches were demonstrated in their comparison. Since then, several attempts have been made to predict the axial and secondary flow patterns inside helicoidal pipes both experimentally and numerically.[10–12]

Most experimental studies have been concerned with the effect of curvature. The experimental data available for convective heat transfer in curved pipes have been influenced by the buoyancy force to varying degrees. In applications where the heat flux is high, the buoyancy force has a significant effect on fluid flow and heat transfer in helicoidal pipes. Numerical investigations examining the combined effects of curvature and buoyancy on fluid flow and heat transfer have been documented by many researchers.[11,13–16] It has been found that the buoyancy force causes the secondary flow pattern to rotate clockwise and the peripheral maximum heat transfer rate location to shift from the outer coil wall to the bottom of the tube cross section in the vertical coil.[17] Some effort has been made to establish a heat transfer regime map and to determine the condition in which both curvature and the buoyancy force are important.[13–15] Futagami and Aoyama[15] used $DePr^{0.5}$ and Ra as parameters to map the heat transfer regime, whereas Lee et al.[14] used De and Gr for a fluid with $Pr = 1$. In Futagami and Aoyama's[15] map, the Prandtl number effect was included so that it could be used for different working fluids.

Few detailed experimental investigations have been conducted on the effect of natural convection on convective heat transfer in helicoidal pipe. Only Abul-Hamayel and Bell[6] reported natural convection to be significant in some of their tests, whereas Cheng and Yuen[18] provided flow visualization pictures of the cross-stream motion. Experimental data with which to verify the numerical results reported in the literature are scarce; therefore, the effect of natural convection on heat transfer inside helicoidal pipes was explored in this investigation.

Experimental System

Experimental Apparatus

Figure 1 presents a schematic representation of the flow loop, featuring the main components and instrumentation. The loop consisted of a main storage tank (100-gal capacity); a $1\frac{1}{4}$-hp, two-speed circulating pump; two sets of flow meters (a large and a small rotameter and vortex and turbine flow meters), an inlet plenum, a test section, an outlet plenum, and a cooling system. The flow rate was adjusted by means of a bypass valve and different valves on the loop, which was measured with a turbine or vortex flow meter. Two plenums were installed before and after the test section in the loop system to dampen the fluid vibration caused by the pump.

To ensure that the working fluid operated under a pressure higher than atmospheric pressure, an additional control valve was placed beyond the exit of the test section, thus preventing air bubble discharges into the test loop. Since air bubbles in the measurement make the flow entirely different from single-phase laminar flow, their elimination is imperative. Beyond the test section, the fluid flowed to a cooling system; it was then mixed with the fluid inside the main tank for recycling. The loop was assembled from a brass pipe 2 in. in diameter. No insulation was placed around the test loop, except for around the test section.

Test Section

The test section consisted of a five-turn helicoidal pipe made of a 304 stainless-steel tube with an i.d. of 22.9 mm and an o.d. of 25.4 mm. The D_c was 259.0 mm, which corresponded to the curvature ratio $D_c/d = 11.3$. The b was 62.5 mm ($D_c/b = 4.1$). Details of the geometry of the test section and thermocouple locations are presented in Fig. 2. Distilled water and ethylene glycol were used as working fluids, with an inlet bulk temperature in the range of 20–30°C and a bulk temperature increase in the range of 10–20°C. The purpose of these restrictions was to limit the fluid property variation. The Ra was limited to a very narrow range for a given De by these restrictions. In the current investigation, the test section was oriented at different angles, which included vertical, inclined, and horizontal positions.

A flow-developing portion of straight pipe ($\sim 120d$) was positioned upstream from the helicoidal pipe test section. This straight portion of pipe provided a well-developed velocity profile at the coil entrance. A dc heating technique was employed by passing high dc through the test section. The current source was a constant voltage/constant current dc arc welder. During the experiments, the tube wall temperature distribution was measured along the heated length using E-type thermocouples that were attached to the outside of the tube wall by epoxy. Starting from the entrance of the coil, four thermocouples were installed at the cross sections after every one-quarter turn except in the third turn, where 72 thermocouples were installed in nine cross sections at an interval of one-eighth turn. The inlet and outlet bulk temperatures were also measured with E-type thermocouples. The inlet temperature was placed in the flow passage upstream from the hydrodynamic entry length, whereas the outlet thermocouple was placed after a specially designed mixing chamber located downstream from the hydrodynamic exit. It should be mentioned that in another investigation of the same test section conducted prior to this experiment, significant effects of the buoyancy force were observed and the fully developed condition was achieved after two turns. However, fewer thermocouples were positioned on the test section, which was heated by a rope heater. To investigate this phenomena more accurately and quantitatively, this revised experiment was designed. Additional thermocouples

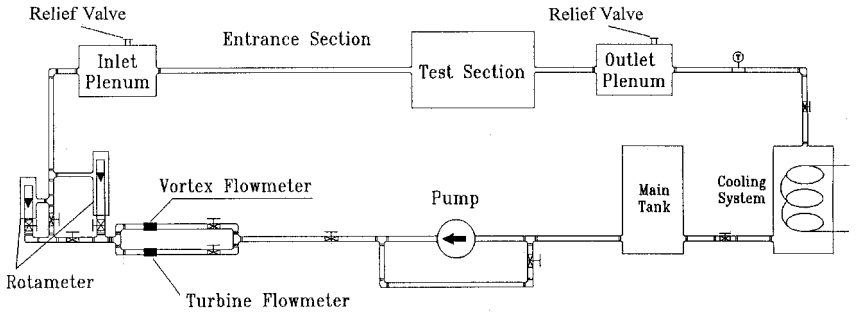

Fig. 1 Schematic representation of the experimental setup.

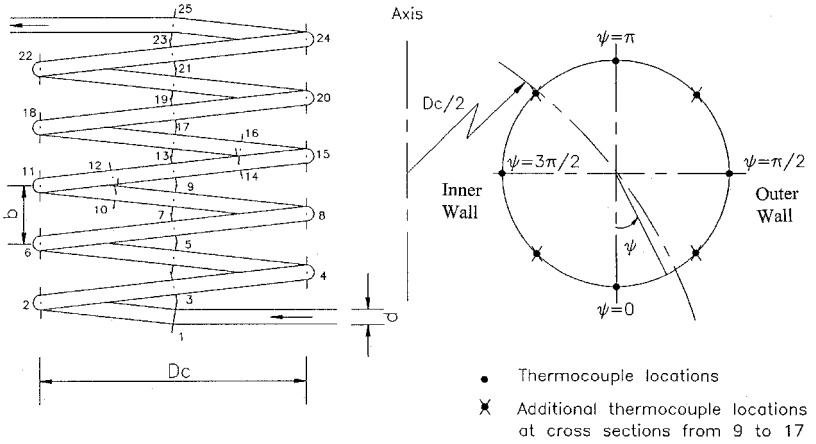

Fig. 2 Schematic representation of the test section.

were installed, especially on the third turn. The heating method was improved by using dc heating on the tube wall.

Before installation, all thermocouples were calibrated using a precision thermometer, with an accuracy of ±0.1°C. After installing all thermocouples, the test section was covered with two layers of one-half-in.-thick fiberglass insulation material. Prior to testing, the insulated helicoidal pipe with the thermocouples was calibrated again in situ at three fixed temperatures between 20–60°C. This recalibration was accomplished by passing preheated water at a high flow rate through the test section without electric heating. Under such conditions, readings of all wall temperatures and the inlet and outlet bulk temperatures should be equal or very similar. The criterion of ±0.2°C was set for all readings. If the difference was higher than that criterion, small corrective differentials, repair, or replacement of the thermocouple were realized. All thermocouples were connected to a Hewlett–Packard data acquisition system and all readings were automatically recorded.

Experimental Uncertainty

Based on the measurements of the different variables, the major uncertainties were determined. Optimized estimates of the fluid property uncertainties at 20–25°C were $\delta\rho/\rho \approx 0.25$, $\delta k/k \approx 1.0$, and $\delta\upsilon/\upsilon \approx 1.0\%$. The volume flow rate was measured by a flow meter specified to have ±0.1% accuracy and a rate of repeatability of 0.2% for the turbine and vortex flow meters. The uncertainty of the mean velocity was estimated to be approximately 1.52% ($\delta U_m/U_m \approx 1.52\%$). The uncertainty of the pipe diameter measurement ($\delta d/d$) was about 2%. Based on a comparison of the electric heating power and a calculation from the bulk temperature increase, the uncertainty of the heat flux calculation ($\delta q''/q''$) was determined to be less than 5%. All thermocouples were calibrated with an accuracy of ±0.1°C. Thus, it was estimated that $\delta(T_w - T_b) \approx \pm 0.2$°C. According to our experimental data, the minimum and maximum temperature differences of $(T_w - T_b)$ were approximately 0.7 and 7.0°C, respectively. For most experiments, the temperature difference $(T_w - T_b)$ was higher than 2.0°C. Therefore, for our experiments, the uncertainties of $\delta Re/Re$, $\delta De/De$, and $\delta Nu/Nu$ were estimated to be less than 2.37, 2.60, and 12.0%, respectively.

Results and Discussion

The effect of natural convection on heat transfer inside horizontal, inclined, and vertical helicoidal pipes has been explored in this investigation. The peripheral and axial wall temperature distributions along the test section were measured on the outside of the tube wall. The inside wall temperatures were calculated from the following equation:

$$T_{wi} = T_{wo} - \frac{q''r_i}{r_o^2 - r_i^2}\left[\ell n\left(\frac{r_o}{r_i}\right) - \frac{1}{2}\right] \tag{4}$$

All of the results presented are based on the inside wall temperatures. θ vs Z is presented to demonstrate the manner in which the flow and heat transfer develops and whether any buoyancy effect is present. In all figures, θ and Z are defined as follows:

$$Z = \frac{z}{L}, \qquad \theta = \frac{(T_w - T_{b,\text{in}})}{(T_{b,\text{out}} - T_{b,\text{in}})} \tag{5}$$

where z denotes the length from the entrance of the helicoidal pipe and $T_{b,\text{out}}$ and $T_{b,\text{in}}$ are the outlet and inlet fluid bulk temperatures, respectively. The peripheral local Nusselt number distribution is also presented to discuss the effect of natural convection on the secondary flow pattern. Finally, the results of the average Nusselt number are discussed.

For the constant heat flux boundary condition, the local Nusselt number is defined as

$$Nu_\psi = \frac{q''d}{k(T_{w,\psi} - T_b)} \tag{6}$$

where $T_{w,\psi}$ represents the local wall temperature and T_b denotes the fluid bulk temperature at the same cross section. It is assumed that T_b increases linearly with flow distance. This assumption is appropriate for determining the heat transfer coefficient in the fully developed region. In the fully developed region, the average Nusselt number can be determined by the following equation:

$$Nu = q''d/k\Delta T_m \tag{7}$$

where ΔT_m is defined as the mean value of $T_w - T_b$ in the fully developed region.

Vertically Oriented Coil

In the axially vertical coil, the flow entered the test section at the bottom and moved upward. In this case, the buoyancy and centrifugal forces were perpendicular to each other at every cross section.

Axial Wall Temperature Distribution

Figure 3 illustrates the wall temperature distribution along the vertically oriented coil for water and ethylene glycol flow, where ψ is defined in Fig. 2. These figures indicate that after the second turn the wall temperature distribution apparently becomes linear as the flow proceeds and is parallel to the fluid bulk temperature distribution. This indicates that the fluid flow and heat transfer can be considered fully developed after two turns.

In the case of pure forced convection, the secondary flow caused by curvature develops in such a pattern that the fluid

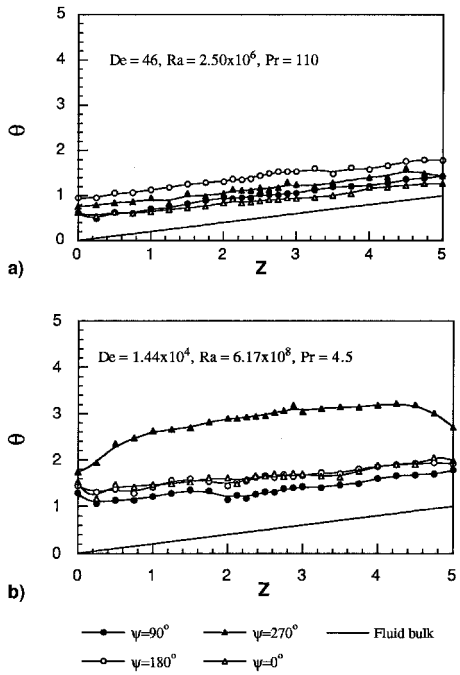

Fig. 3 Dimensionless axial temperature distributions for the vertically oriented coil.

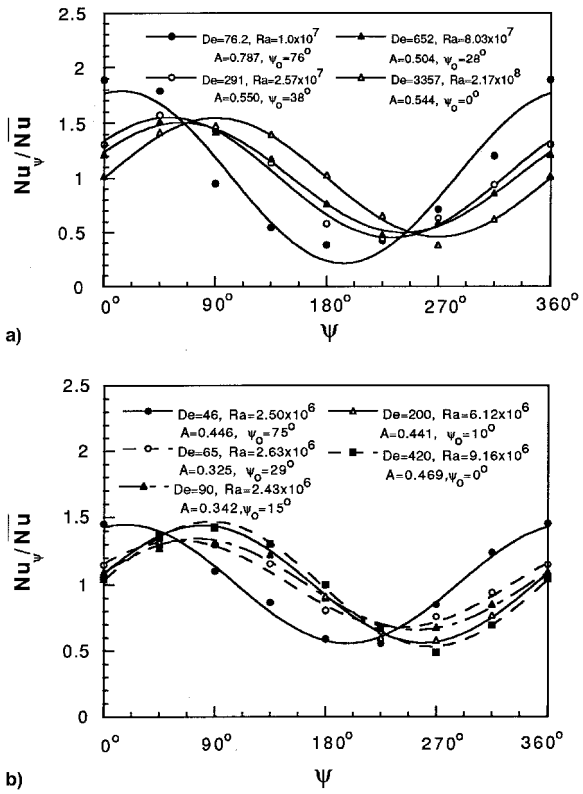

Fig. 4 Peripheral relative Nusselt number distributions for the vertically oriented coil: a) water flow (*Pr* = 4.5) and b) ethylene glycol flow (*Pr* = 110).

moves from the inner wall to the outer wall through the core of the cross section and flows back to the inner wall along the tube wall. It creates the highest heat transfer coefficient on the outer wall (ψ = 90 deg) and the lowest heat transfer coefficient on the inner wall (ψ = 270 deg). Thus, the temperatures on the outer and inner walls should be the lowest and highest, respectively, over the tube circumference.

Our experimental data show that when the Dean number is lower (Fig. 3a), the temperature on the top of the cross section of the coil (ψ = 180 deg) is higher than that on the inner wall (ψ = 270 deg), and the temperature on the bottom (ψ = 0 deg) is lower than that on the outer wall (ψ = 90 deg). This can be attributed to the fact that the natural convection causes the secondary flow pattern to rotate clockwise, a phenomenon that has been predicted by numerous numerical studies[11,14,15] and is clearly evident from the peripheral Nusselt number distribution discussed in the next section. As the Dean number increases, the natural convection effect decreases. When the Dean number is high enough, the inner coil wall temperature becomes the highest, and the outer coil wall temperature becomes the lowest. In addition, the temperatures at the top and bottom of the cross section are in between those at the inner and outer coil walls and approximately the same as seen in Fig. 3b. This indicates that the curvature effect dominates the secondary flow in the high Dean number flow.

Figure 3 shows that for a higher Prandtl number fluid flow, the overall dimensionless wall temperature distributions are much higher than those for the lower Prandtl number fluid flow. This suggests that as the Prandtl number increases, the peripheral temperature variation becomes stronger for the uniform heat flux boundary condition.

Peripheral Nusselt Number Distribution

Demonstrating the effect of natural convection on the peripheral local heat transfer characteristics, Fig. 4 shows the peripheral variations of the relative local Nusselt number, $Nu_\psi/\overline{Nu}$, in the fully developed region (Z = 2.5) for the water and ethylene glycol flows. Nu_ψ is the local peripheral Nusselt number at the angle of ψ. The relative local Nusselt number distribution vs ψ can be correlated by the following function:

$$Nu_\psi/\overline{Nu} = 1 + A \sin(\psi + \psi_0) \qquad (8)$$

where A and ψ_0 are correlation constants. The value of A represents the amplitude of the peripheral variation, whereas ψ_0 represents the shift of the locations of the maximum and minimum Nusselt number. The values of A and ψ_0 for different cases are provided in Fig. 4.

As indicated in Fig. 4, for a high Dean number flow (water flow with De = 3357, Ra = 2.17 × 10^8 and ethylene glycol flow with De = 420, Ra = 9.16 × 10^6), the maximum and minimum peripheral Nusselt numbers are located at the outer coil wall (ψ = 90 deg) and the inner coil wall (ψ = 270 deg), respectively. This suggests that the secondary flow is dominated by centrifugal force. As the Dean number decreases with a slight change in the Ra, the maximum peripheral Nusselt number location shifts from ψ = 90 to 0 deg, whereas the minimum peripheral Nusselt number location gradually shifts from ψ = 270 to 180 deg. This variation is well illustrated by the variation of the value of ψ_0. For example, for water flow in the case of De = 76 and Ra = 1.0 × 10^7 and in the case of De = 3357, Ra = 2.17 × 10^8, ψ_0 is approximately equal to 76 and 0 deg, respectively. It can be concluded that the natural convection existing in the low Dean number flow causes the rotation of the secondary flow patterns, a conclusion that agrees well with the numerical predictions.[11,14,15,17]

A careful examination of the values of A in Fig. 4 demonstrates that as the De increases, the peripheral variation of the relative Nusselt number A decreases and then increases. The increase of the Dean number has two effects. First, the secondary flow caused by centrifugal force becomes stronger. At the same time, natural convection is suppressed. For the lower Dean number flow, in which natural convection is important to the secondary flow, the second effect overwhelms the first. For a higher Dean number flow, where centrifugal force dominates the secondary flow, the first effect is significant and the peripheral variation of the relative Nusselt number becomes stronger.

As previously mentioned, the Ra was limited to a narrow range for a given De by a restriction of the experimental con-

ditions. It is difficult to maintain the same *De* and *Ra* for different fluids. However, a careful examination of the results reveals that for a higher Prandtl number fluid flow (ethylene glycol), the natural convection effect is present in the lower *De* region.

Heat Transfer Regimes

The combined influences of centrifugal and buoyancy forces have been investigated by several researchers.[13–17] Heat transfer inside curved and helicoidal pipes is classified into three regimes: 1) a regime in which centrifugal force is dominant, 2) a regime in which centrifugal force and buoyancy force are effective (the composite regime), and 3) a regime in which buoyancy force is dominant. In a previous numerical study,[15] the boundaries between different heat transfer regimes were defined by comparing the average Nusselt number with that of pure forced or pure natural convection using a criterion of 2% variation of the average Nusselt number.

The present experimental results show that although the local Nusselt number distributions are significantly affected by natural convection in such a way that the locations of the highest and lowest Nusselt numbers shift, the average is barely affected. In this study, the heat transfer regime was defined by the location of the maximum peripheral Nusselt number. If the maximum peripheral Nusselt number was located in the range ψ = 15–75 deg, the flow was considered to be in the mixed regime (2). When ψ > 75 deg or ψ < 15 deg, the flow was considered to be in regime 1 or 3, respectively. In Fig. 5 present experimental findings are compared with the heat transfer regime map based on numerical work.[15] It can be observed that our results agree fairly well with the previous data. Some deviations between the experimental and numerical results can also be seen in Fig. 5. These deviations may result from the different methods used to define the regime boundaries.

Horizontal and Inclined Coils

For horizontal and inclined coils, the fluid entered the test section horizontally from the top of the first turn, where *Z* = 0. The fluid descended in the first half-turn and ascended in the second half-turn, etc. Since the direction of natural convection is always from the bottom of the test section to the top, the natural convection is periodically counter and parallel to the main flow in the coils. Thus, the interaction between natural convection and the curvature induced secondary flow changes along the flow direction periodically. As a result, the flow structure in horizontal or inclined coil is very complex when the buoyancy force is effective.

Axial Wall Temperature Distribution

Figure 6 illustrates the dimensionless tube wall temperature distribution along the main flow direction in the horizontal coil. It can be seen in Figs. 6a and 6b that for the low Dean number flow, the tube wall temperature is periodically wavy.

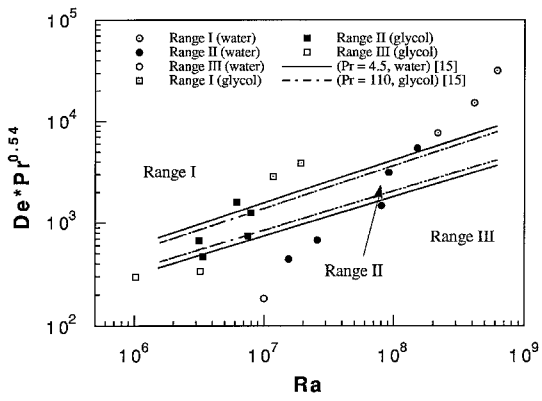

Fig. 5 Heat transfer regimes.

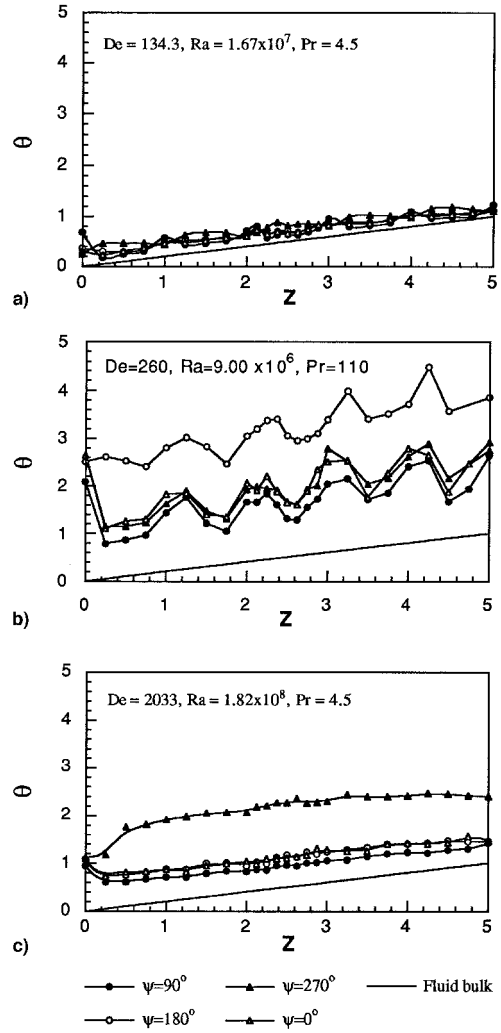

Fig. 6 Dimensionless axial temperature distributions for the horizontally oriented coil.

It is believed that this phenomena is caused by natural convection that periodically occurs along and against the main flow. At locations ψ = 0, 90, and 180°C, the temperatures decrease in the first half of each turn, where natural convection opposes the main flow, and increase in the second half of each turn of the flow direction, where natural convection corresponds to the main flow. For a very low *De* (Fig. 6a), the temperature of the outer coil wall at the top of each turn achieves the highest value of the cross section, where natural convection occurs in the plane of the cross section and overwhelms the secondary flow caused by the curvature.

For the higher *De* flow, the temperature distributions along the test section become smoother. After two turns, the wall temperature distributions approach straight lines, and the effect of the natural convection disappears (Fig. 6c), similar to the cases for the vertically oriented coil discussed previously. The results reveal that the fluctuation of the wall temperature along the flow direction is stronger for a high Prandtl number fluid flow (ethylene glycol) than for a low Prandtl number fluid flow (water), even though the *Ra* for a higher Prandtl number fluid is lower than that for the lower Prandtl number fluid. Comparing Figs. 6a and 6c indicate that as the Dean number increases, natural convection becomes increasingly suppressed. The higher the Prandtl number, the more intensive the effect of natural convection on the temperature distributions.

Peripheral Nusselt Number Distribution

As examples, Fig. 7 depicts some relative peripheral Nusselt number distributions at different cross sections of the third turn

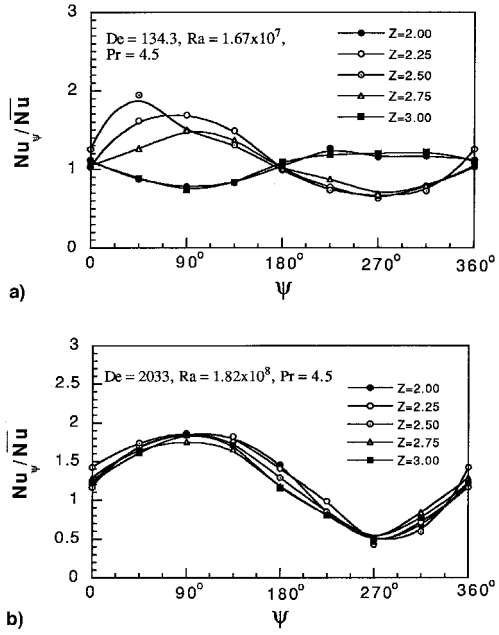

Fig. 7 Peripheral relative Nusselt number distributions for the horizontally oriented coil.

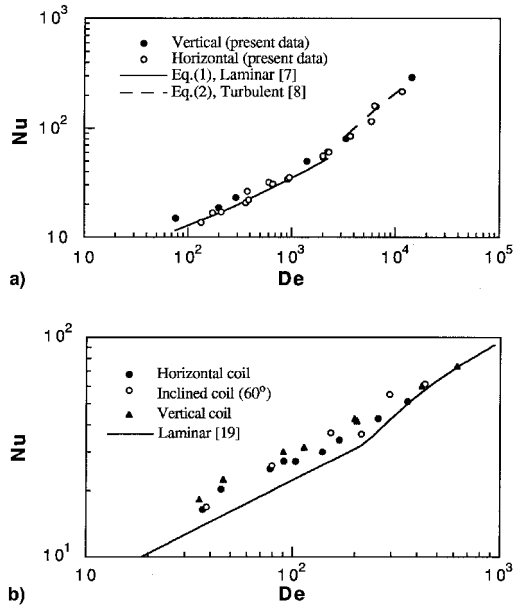

Fig. 8 Average Nusselt number and comparison: a) water flow and b) ethylene glycol flow.

for the water flow. An examination of Figs. 6 and 7 reveals that the flow and heat transfer behaviors tend to repeat themselves along the coil periodically after the second turn ($Z > 2.0$). Therefore, based on this phenomenon, the concept of periodically fully developed flow and heat transfer is introduced. The same distributions at the beginning and at the end of the third turn ($Z = 2.0$ and 3.0) indicate that the flow and heat transfer are fully developed. For low Dean number flow, the peripheral distribution of the relative Nusselt number at the top is reversed relative to the other cross sections, and the locations of the peripheral maximum and minimum Nusselt numbers are also reversed (Fig. 7a). This indicates that natural convection overwhelms the secondary flow caused by the curvature at the top of each turn. As the Dean number increases, the buoyancy effect is suppressed, and the differences among the peripheral distributions at different cross sections decrease and then vanish as the *De* becomes high enough (Fig. 7b).

The same distribution behavior is observed for the ethylene glycol flow, except that the amplitude of the peripheral variation of the Nusselt number is larger.

Effect of the Inclination Angle

To examine the effect of the inclination angle, the test section with an inclination angle of 60 deg from horizontal was tested for the ethylene glycol flow. The experimental results show that the temperature distributions for the inclined coil are similar to those found in the horizontally oriented coil, the only difference being that the wavy amplitude along the flow direction for the inclined coil is a little smaller than that for the horizontal coil. Similar behaviors for the peripheral relative Nusselt number distributions were observed for the inclined coil, but with a smaller peripheral variation of amplitude. This implies that as the inclination angle increases, the effect of natural convection decreases and is minimized as the inclination approaches the vertical orientation.

Average Nusselt Number

The average Nusselt numbers of the fully developed and periodically fully developed regions are plotted in Fig. 8. For the water flow, our experimental findings are compared to the empirical correlations [Eqs. (1) and (2)] provided in Manlapaz and Churchill[7] and Gnielinski.[8] Inasmuch as the experimental data for fluids with a high Prandtl number do not adequately apply to these two correlations,[19] the data for the high Prandtl number fluid (glycol) are compared with our previous forced convection experimental results for ethylene glycol in one-half-in. helicoidal pipes.[19] The comparison indicates that although natural convection exists and has a significant effect on the wall temperature distributions and the local peripheral Nusselt numbers, the average Nusselt numbers in the fully developed and periodically fully developed regions are still similar to the results obtained in the case of forced convection. It can be observed that for high Prandtl number fluid flow (ethylene glycol), the average Nusselt number increases up to 20% in our experimental range, and for both water and ethylene glycol flows, the results for the horizontally oriented coil are slightly lower than those for the vertically oriented coil. It can be concluded that because of the existence of natural convection in the low Dean number flow, natural convection enhances heat transfer within the helicoidal pipe. As the Prandtl number increases, this enhancement of the heat transfer becomes more pronounced.

Concluding Remarks

The effect of natural convection on convective heat transfer in a helicoidal pipe has been investigated in this experimental investigation. Vertically oriented, inclined, and horizontally oriented coils were tested. The following conclusions have been drawn from the experimental results:

1) For the vertically oriented coil, the flow and heat transfer approach fully developed after two turns, although natural convection causes the location of the peripheral maximum Nusselt number to shift from the outer wall to the bottom of the cross section.

2) The relative local peripheral Nusselt number distributions are well correlated in the form of Eq. (8). The variations of the values of A and ψ_0 indicate that natural convection causes the secondary flow pattern to rotate clockwise for the vertical coil. The experimental results agree fairly well with the heat transfer regime map found in the open literature.

3) For the horizontally oriented coil, natural convection causes the temperature distribution along the coil to become periodically wavy. The flow and heat transfer can be considered periodically fully developed after two turns. As the Dean number increases, natural convection is suppressed, and the wall temperature distributions along the flow direction become smoother (i.e., the wavy behaviors of the wall temperature distributions disappear).

4) The amplitude of the wavy temperature distributions decreases when the inclined coil angle increases from the horizontal orientation, indicating that the effect of natural convection is diminished. The variation of the local peripheral Nusselt number along the peripheral angle infers the same conclusion.

5) Although natural convection has a significant effect on the wall temperature distributions and the local Nusselt number, the average Nusselt number of the fully developed or the periodically fully developed flow for the fluid with the lower Prandtl number (water) is affected only slightly, whereas for the higher Prandtl number fluid flow (ethylene glycol), the average Nusselt number increases up to 20% in our experimental range. The higher the Prandtl number, the more significant is the effect of natural convection on both the local and the average Nusselt numbers.

Acknowledgments

The results presented in this paper were obtained in the course of research sponsored by the National Science Foundation. The authors would like to thank Walter Conklin and Julian Black for their assistance during the power supply installation and experiments.

References

[1]Berger, S. A., and Talbot, L., "Flow in Curved Pipes," *Annual Review of Fluid Mechanics*, Vol. 15, 1983, pp. 461–512.

[2]Seban, R. A., and McLaughlin, E. F., "Heat Transfer in Tube Coils with Laminar and Turbulent Flow," *International Journal of Heat and Mass Transfer*, Vol. 6, No. 5, 1963, pp. 387–395.

[3]Mori, Y., and Nakayama, W., "Study on Forced Convective Heat Transfer in Curved Pipes (1st Report, Laminar Region)," *International Journal of Heat and Mass Transfer*, Vol. 8, No. 1, 1965, pp. 67–82.

[4]Schmidt, E. F., "Waermeuebergang und Druckverlust in Rohrschlangen," *Chemie-Ingenieur-Technik*, Vol. 39, No. 13, 1967, pp. 781–789.

[5]Dravid, A. N., Smith, K. A., Merrill, E. W., and Blian, P. L. T., "Effect of Secondary Fluid Motion on Laminar Flow Heat Transfer in Helically Coiled Tubes," *AIChE Journal*, Vol. 17, No. 5, 1971, pp. 1114–1122.

[6]Abul-Hamayel, M. A., and Bell, K. J., "Heat Transfer in Helically Coiled Tubes with Laminar Flow," American Society of Mechanical Engineers, Paper 79-WA/HT-11, Nov. 1979.

[7]Manlapaz, R. L., and Churchill, S. W., "Fully Developed Laminar Convection from a Helical Coil," *Chemical Engineering Communication*, Vol. 9, Nos. 1–6, 1981, pp. 185–200.

[8]Gnielinski, V., "Heat Transfer and Pressure Drop in Helically Coiled Tubes," *Proceedings of the 8th International Heat Transfer Conference*, Vol. 6, Taylor and Francis, Washington, DC, 1986, pp. 2847–2854.

[9]Austen, D. S., and Soliman, H. M., "Laminar Flow and Heat Transfer in Helically Coiled Tubes with Substantial Pitch," *Experimental Thermal and Fluid Science*, Vol. 1, No. 2, 1988, pp. 183–194.

[10]Yang, G., and Ebadian, M. A., "Convective Heat Transfer in a Curved Annular Sector Duct," *Journal of Thermophysics and Heat Transfer*, Vol. 7, No. 3, 1993, pp. 441–446.

[11]Yang, G., and Ebadian, M. A., "Mixed Convective Flow and Heat Transfer in a Vertical Helicoidal Pipe with Finite Pitch," *Computational Mechanics*, Vol. 14, No. 5, 1994, pp. 503–513.

[12]Yang, R., and Chang, S. F., "A Numerical Study of Fully Developed Laminar Flow and Heat Transfer in a Curved Pipe with an Arbitrary Curvature Ratio," *International Journal of Heat and Fluid Flow*, Vol. 14, No. 1, 1993, pp. 138–145.

[13]Prusa, J., and Yao, L. S., "Numerical Solution for Fully Developed Flow in Heated Curved Tubes," *Journal of Fluid Mechanics*, Vol. 123, Oct. 1982, pp. 503–522.

[14]Lee, J.-B., Simon, H. A., and Chow, J. C. F., "Buoyancy in Developed Laminar Curved Tube Flows," *International Journal of Heat and Mass Transfer*, Vol. 28, No. 3, 1985, pp. 631–640.

[15]Futagami, K., and Aoyama, Y., "Laminar Heat Transfer in a Helically Coiled Tube," *International Journal of Heat and Mass Transfer*, Vol. 31, No. 2, 1988, pp. 387–396.

[16]Goering, D. J., "The Influence of Curvature and Buoyancy in Three-Dimensional Pipe Flows," Ph.D. Dissertation, Univ. of California, Berkeley, CA, 1989.

[17]Yao, L. S., and Berger, S. A., "Flow in Heated Curved Pipes," *Journal of Fluid Mechanics*, Vol. 88, Pt. 2, 1978, pp. 339–354.

[18]Cheng, K. C., and Yuen, F. P., "Flow Visualization Experiments on the Secondary Flow Pattern in an Isothermally Heated Curved Pipe," *Journal of Heat Transfer*, Vol. 109, No. 1, 1987, pp. 55–61.

[19]Xin, R. C., Bendana, J., Li, W., and Ebadian, M. A., "The Effects of the Prandtl Number and Torsion on Convective Heat Transfer in Helicoidal Pipes," *Fundamentals of Heat Transfer in Forced Convection*, American Society of Mechanical Engineers, Heat Transfer Div., HTD-V. 285, 1994, pp. 85–92.